Applied Radiation and Isotopes 202 (2023) 111070

Contents lists available at ScienceDirect

Applied Radiation and Isotopes

journal homepage: www.elsevier.com/locate/apradiso

Primary standardization and Monte Carlo modeling of (^{243}Am + ^{239}Np) by means of a 4π(PC)-γ coincidence counting system

Marina F. Koskinas, Denise S. Moreira, Ione M. Yamazaki, Marcelo Colonno, Renato Semmler, Thales S.L. Morais, Mauro S. Dias *

Instituto de Pesquisas Energéticas e Nucleares, IPEN-CNEN/SP, Av. Prof. Lineu Prestes 2242, 05508-000, São Paulo, SP, Brazil

ARTICLE INFO

Keywords:
^{243}Am + ^{239}Np
Coincidence system
Disintegration rate
Monte Carlo simulation

ABSTRACT

The procedure followed by the Nuclear Metrology Laboratory (LMN) at the IPEN for the primary standardization of a (^{243}Am + ^{239}Np) solution, in secular equilibrium, is described. The measurement was carried out in a 4π(PC) (α,β)−γ coincidence system. The total activity per unit mass of the solution was determined by the extrapolation technique, using a software coincidence counting systsem. The extrapolation curves were compared with Monte Carlo calculations by means of Code ESQUEMA, used in previous works, which, was improved and applied in order to calculate the alpha, beta, gamma, X-rays and coincidence spectra.

1. Introduction

The Nuclear Metrology Laboratory (*Laboratório de Metrologia Nuclear* - LMN) at the IPEN in Sao Paulo (Brazil) has developed primary standardization methods for determining the activity of several radionuclides such as ^{64}Cu (Yamazaki et al., 2018), ^{166}Ho (Yamazaki et al., 2020) and ^{59}Fe (Koskinas et al., 2016). In this paper, (^{243}Am + ^{239}Np) standardization methodology using a 4π(PC) (α,β)−γ coincidence system composed of gas-flow 4π proportional counter coupled to one NaI (Tl) scintillation counter is presented.

In the present experiment, an (^{243}Am + ^{239}Np) solution in secular equilibrium was used. ^{243}Am is an important radionuclide to be used in determining the radioactivity of alpha emitters by alpha–ray spectrometry. The ^{243}Am is used as a chemical yield tracer in many chemical analysis applications, to account for the recovery of the alpha particle emitting radionuclide, as the case of ^{241}Am present as an impurity in radiopharmaceutical solutions, such as ^{99}Mo, usually produced by fission using enriched uranium-235. In addition, it is used to determine the presence of ^{241}Am in environmental waste from nuclear power plants.

The ^{243}Am decays almost 100% by alpha transitions (with a very small branch, 10-9 %, of spontaneous fission), to ^{239}Np with a Q_α value of 5438.8 keV, and a half-life of 7367(23) years. Most of the decay (86.74 %) populates the excited level of ^{239}Np, with energy of 74.66 keV. The alpha decay is followed by a beta decay from ^{239}Np to ^{239}Pu, with a Q_β of 722.5 keV, and a half-life of 2.356(3) days, populating mainly the excited levels of 228.18 keV (38.6 %) and 277.59 keV (34.8 %) of ^{239}Pu, as shown in simplified decay scheme Fig. 1 (Bé, M.-M. et al., 2006, 2008).

The activity per unit mass of the solution was determined by the extrapolation technique. Cox-Isham formalism (Cox and Isham, 1977) was applied to experimental data and all partial uncertainties were considered applying the covariance analysis methodology.

A Monte Carlo simulation by means of an improved version of code ESQUEMA, developed by Takeda et al. (2005) and Dias et al. (2013), was used. In this code the detector responses were obtained by applying code MCNP6 (ORNL, 2013), and considering all aspects of the counting system, including the radioactive source and absorbers details. The code, ESQUEMA, was modified to calculate the alpha, beta, gamma, X-rays and coincidence spectra, taking into account the decay scheme information (Bé, M.-M. et al., 2006, 2008). This provided an independent comparison with the experimental results.

2. Experimental method

2.1. Source preparation

The (^{243}Am + ^{239}Np) solution was obtained from the LNMRI (*Laboratório Nacional de Metrologia de Radiações Ionizantes*), in Rio de Janeiro, and the chemical composition was HCl, 0.1M. There were no detectable

* Corresponding author. Instituto de Pesquisas Energéticas e Nucleares, IPEN-CNEN/SP, Centro do Reator de Pesquisas (CRPq), Av. Prof. Lineu Prestes 2242, 05508000, São Paulo, SP, Brazil.
E-mail address: msdias@ipen.br (M.S. Dias).

https://doi.org/10.1016/j.apradiso.2023.111070
Received 29 May 2023; Received in revised form 14 September 2023; Accepted 9 October 2023
Available online 10 October 2023

impurities, as reported by the LNMRI (da Silva et al., 2012). This solution was used more than 10 years after production. Therefore, the assumption of secular equilibrium is satisfied.

The sources were prepared by dropping known aliquots of the solution on a 20 μg cm^{-2} thick Collodion film. This film had been previously coated on each side with 10 μg cm^{-2} gold layers, in order to render the film conductive. A seeding agent (CYASTAT SM) was used to improve the deposit uniformity and the sources were dried in a dissecator. The pycnometer technique (Campion, 1975) using a Mettler 56XP balance performed the mass determination. A total of 8 sources were prepared with masses ranging from 10 mg to 51 mg.

Some of these sources were measured in the HPGe gamma-ray spectrometer for impurity checks and no impurities were detected.

2.2. $4\pi\alpha\beta-\gamma$ coincidence method

A 4π proportional counter filled with P-10 gas and operated at 0.1 MPa was used for alpha and beta detection. Its outside wall (with a 0.1 mm thick Al window) was coupled to the crystal scintillator, in order to minimize gamma-ray attenuation. The detector was a 76 mm × 76 mm NaI(Tl) crystal.

The (^{243}Am + ^{239}Np) source activities were determined by the extrapolation method from data acquired with two gamma windows covering the 75 keV total energy absorption peak in coincidence with the ^{243}Am alpha decay and another one at (228 + 278) keV, covering the 228 and 278 keV total energy absorption peaks, in coincidence with the ^{239}Np, and corresponding to the beta decay.

The measurements were performed at two detector bias: one at 1.45 kV and another one at 1.80 kV. In both cases, the **4π** detector was able to measure **α** particles and electrons. For the higher bias, the alpha

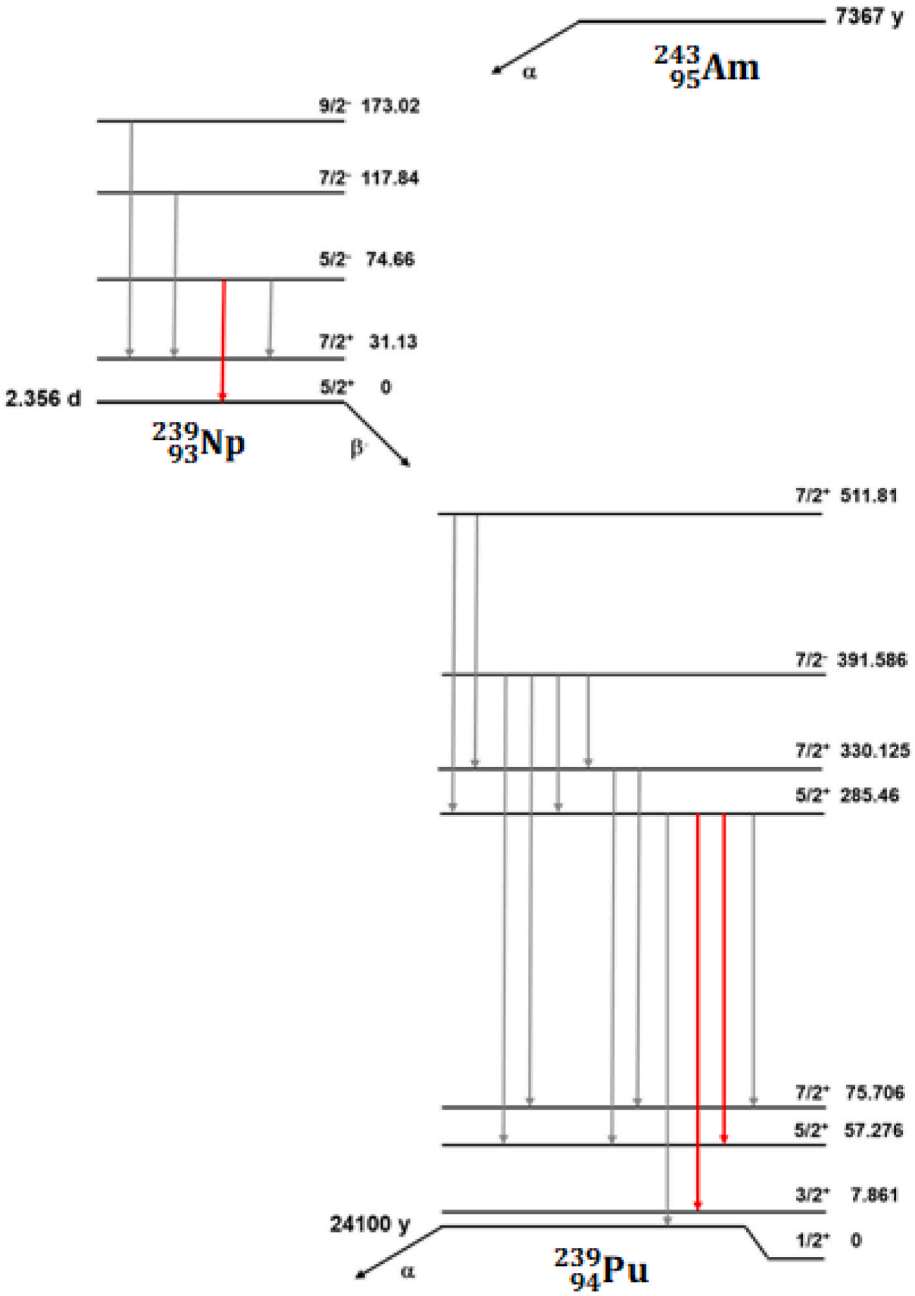

Fig. 1. Simplified decay scheme of (^{243}Am + ^{239}Np). All the energies are in keV (Bé et al., 2006, 2008).

spectrum was over saturated. However, in this condition the measurements could achieve much higher beta efficiencies. Therefore, the extrapolation value, shown by Eq. (1), is expected to be $2N_0$, in both cases. The variation of alpha and beta efficiencies was performed by applying absorbers made of 50 μg cm^{-2} Collodion films coated with gold layers and 200 μg cm^{-2} aluminum foils placed over and under the radioactive sources. The maximum absorber thickness was around 1200 μg cm^{-2}.

The events were recorded by a software coincidence counting system (SCS), developed by the LMN (Toledo et al., 2007). This system digitalizes both alpha/beta and gamma amplifier outputs, registering the pulse height and the occurrence time for all pulses. It is based on a National Instruments PCI-6132 card (National Instruments, 2014). The activity calculation was performed by means of code SCTAC version 6.0 (Dias, 2010), developed at the LMN, which allows the gamma-ray window selection offline, after the data acquisition is finished. The dead time was fixed by software to the value of 6.0 μs. The resolving time was 2.0 μs and considered large enough to account for the 193 ns delayed state at 391.6 keV, which has significant beta feeding. Corrections for dead time and accidental coincidences were applied during the analysis, after the experiment has been completed.

2.3. Coincidence equations

The total counts in the 4π detector can be given by (Woods et al., 1996):

$$N_{(\alpha+\beta)} = N_0[2 + k_1(1 - E_1) + k_2(1 - E_2)] \quad (1)$$

Where:

N_0 corresponds to the individual radionuclide activities, which are equal for ^{243}Am and ^{239}Np, because they are in secular equilibrium. This condition explains the factor 2 inside the brackets;

$E_1 = \frac{N_c}{N_{\gamma 1}}$, $E_2 = \frac{N_c}{N_{\gamma 2}}$ and k_1 and k_2 are constants, given by (Woods et al., 1996)

$$k_1 = \frac{1}{A}\left[1 - \sum_i \left(\frac{\alpha_i \bullet \varepsilon_{ci} + \varepsilon_{\beta\gamma i}}{1 + \alpha_i}\right)\right] \quad (2)$$

and

$$k_2 = \frac{B}{A}\left[1 - \sum_i \left(\frac{\alpha_i \bullet \varepsilon_{ci} + \varepsilon_{\beta\gamma i}}{1 + \alpha_i}\right)\right] - \left[1 - \sum_j \left(\frac{\alpha_j \bullet \varepsilon_{cj} + \varepsilon_{\beta\gamma j}}{1 + \alpha_j}\right)\right] \quad (3)$$

Indexes i and j correspond to the ^{243}Am and ^{239}Np decay transitions, respectively. Eqs. (2) and (3) were modified with respect to those given in reference (Woods et al., 1996) by including the conversion electrons from both radionuclides which are present and contribute substantially to the 4π detector counts.

The reason that can justify the inclusion of conversion electrons in Eqs. (2) and (3), which is a common procedure in writing coincidence equations, is the fact that for some measurements performed at the 75 keV gamma window (^{243}Am alpha decay), the counts reached values near 98–99% of the total activity ($2N_0$). These points were obtained at 1.45 kV, just above the alpha plateau, but still measuring electrons in the 4π detector. This behavior is shown by the left extrapolation curve in Fig. 5 (alpha window). On the other hand, placing the gamma window at (228 + 278) keV (^{239}Np beta decay), and applying a 1.45 kV bias to the 4π detector, the observed beta efficiency (E_2) was very low, around 20%. This was expected because, at this voltage, the pulse amplitudes for low energy beta rays are very low. Considering that E_2 does not account for conversion electrons, this high **4π** detector total counting rate, near $2N_0$, can only be explained by the contribution of conversion electrons, which are not in coincidence with the beta rays from ^{239}Np, but are contributing to the total number of counts. An additional evidence of this effect is the presence of several X-rays in the NaI(Tl) spectrum, as predicted by the Monte Carlo simulation with 1.0 keV energy resolution, which come from these internal conversion transitions from ^{239}Pu, daughter of ^{239}Np.

Parameters A and B can be given by (Woods et al., 1996):

$$A = \frac{\varepsilon_{\gamma 1}}{\varepsilon_{\gamma 1} + a\varepsilon_{\gamma 2}} \quad (4)$$

and

$$B = \frac{a\varepsilon_{\gamma 2}}{\varepsilon_{\gamma 1} + a\varepsilon_{\gamma 2}} \quad (5)$$

Where a is the contribution from the counts of the 106 keV beta decay peak to the 75 keV alpha decay peak.

2.4. Monte Carlo simulation

The theoretical response functions of each detector have been calculated applying MCNP6 Monte Carlo code (Werner et al., 2018). A full description of the 4π(PC) (α,β)−γ system was developed, including details of source substrate and absorbers. Fig. 2 shows the simulation model as depicted by code VISED, which is included in the MCNP6 package. An energy range from 1.4 keV up to 4 MeV has been selected for electrons in the 4π detector, for 196 energy bins, in a stepwise scale. For alpha particles, the energy range was from 4.8 to 6.0 MeV in 61 bins, in linear scale. These two series were repeated 40 times, changing the absorber thickness over and under the sources in order to simulate the experimental foiling process. For gamma-rays the energy range was from 12 to 760 keV in 748 uniform energy bins. The numbers of histories followed for electrons and alphas was 1×10^5 and for gamma-rays 2×10^6, respectively.

Code ESQUEMA, developed at the LMN, has been improved in order to include alpha detection in the 4π proportional counter, needed for the present simulation. All details in the decay scheme were considered in the simulation, applying data from the recommended literature (Bé, M.-M. et al., 2006, 2008). As a result, the code was able to obtain the alpha, beta, gamma and X-ray spectra, and compare with experimental data. This code was also used for calculating the extrapolation curve in the 4π (PC) (α,β)−γ coincidence experiment. In this way, Eq. (1) could be reproduced theoretically as a function of the alpha and beta efficiencies, for each gamma-ray window, gated at 75 keV and (228 + 278) keV, respectively, and compared with the experimental ones.

The final activity value N_0 was obtained by a Least Square fitting procedure, considering the following Chi-Square value:

$$\chi^2 = \left(\vec{y}_{exp} - 2N_0\ \vec{y}_{MC}\right)^T V^{-1} \left(\vec{y}_{exp} - 2N_0\ \vec{y}_{MC}\right) \quad (6)$$

Where:

$\vec{y}_{exp}$ is the experimental vector of $N_{(\alpha+\beta)}$ as a function of (1-E);

$\vec{y}_{MC}$ is the $N_{(\alpha+\beta)}$ vector calculated by Monte Carlo for unitary activity for the same (1-E) value;

$2N_0$ is the radioactive source total activity;

V is the total covariance matrix, including both experimental and calculated uncertainties, and.

T stands for matrix transposition.

A series of simulated values are calculated for a wide range of beta efficiency parameter in small bin intervals. The theoretical value to be used in Eq. (1) is obtained by linear interpolation, for the same corresponding experimental efficiency.

Eq. (4) is applicable when there is only one extrapolation curve. In the present case, there are two theoretical normalized curves that must match each other to the value 1 at $(1-E) = 0$. Moreover, it was observed that a quadratic curve results in a better fit for the beta decay curve. The corresponding least square equation to satisfy these two conditions is given by:

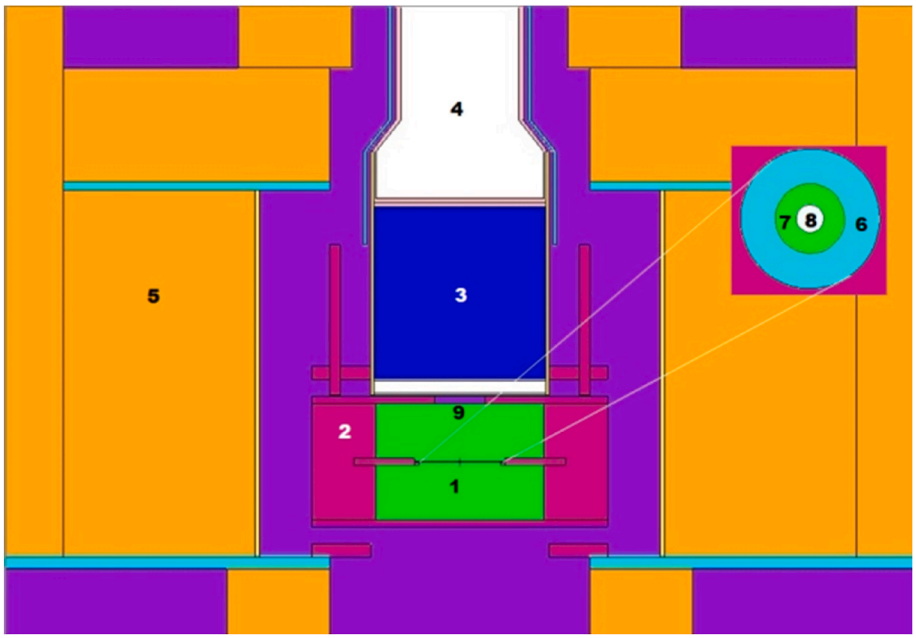

Fig. 2. Image as depicted by code VISED. 1: P-10 filling gas; 2: Brass proportional counter; 3: NaI(Tl) crystal; 4: PMT; 5: Pb shield; 6: stainless steel source holder; 7: Collodion film; 8: source substrate.

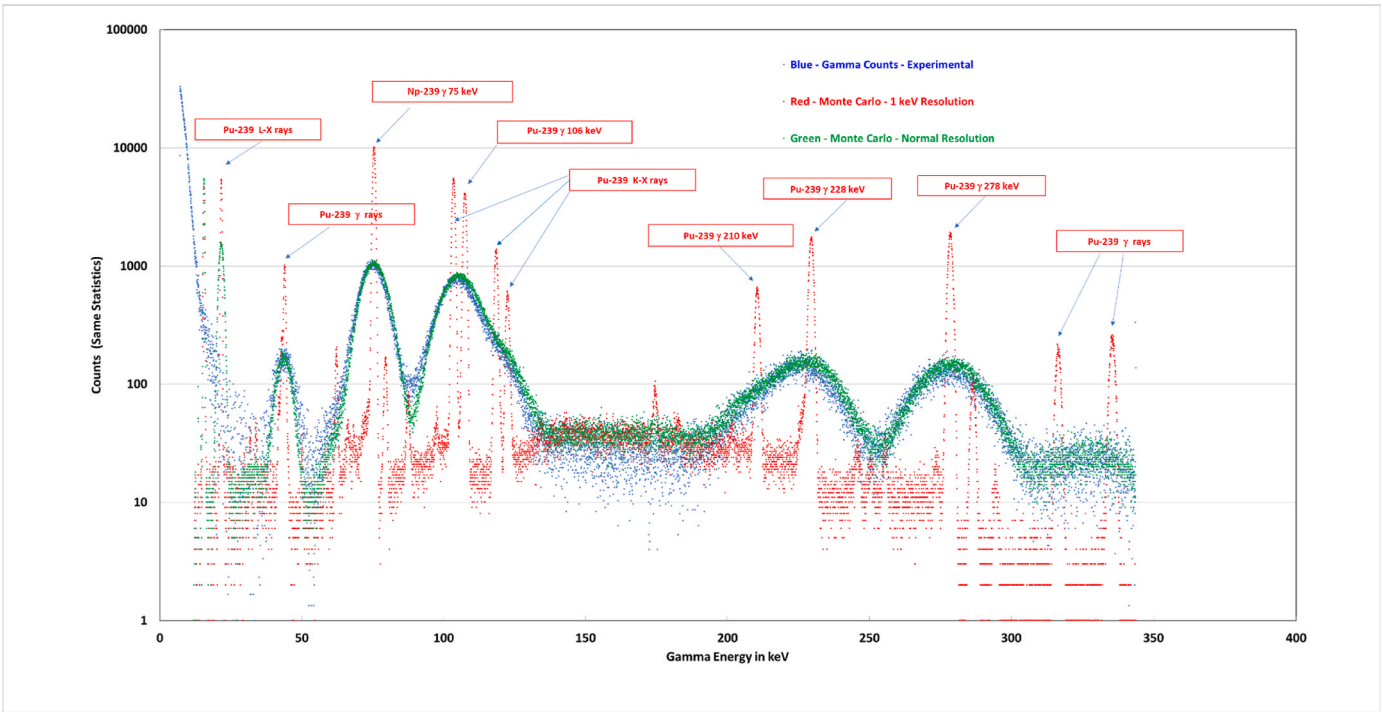

Fig. 3. Gamma-ray spectra comparing experimental results and Monte Carlo calculation. The blue points are experimental data; the green points are Monte Carlo predictions for an energy resolution similar to the experiment. The red points are Monte Carlo predictions for 1 keV energy resolution. In this case, it is possible to identify several X-ray and gamma-ray lines presented in the decay scheme, which were correctly predicted by Monte Carlo simulation.

$$\begin{bmatrix} y_{11} \\ \vdots \\ y_{1m} \\ y_{21} \\ \vdots \\ y_{2n} \end{bmatrix} = \begin{bmatrix} & & & \\ 1 & x_{11} & 0 & 0 \\ \vdots & \vdots & \vdots & \vdots \\ 1 & x_{1m} & 0 & 0 \\ 1 & 0 & x_{21} & x_{21}^2 \\ \vdots & \vdots & \vdots & \vdots \\ 1 & 0 & x_{2n} & x_{2n}^2 \\ & & & \end{bmatrix} \cdot \begin{bmatrix} a \\ b_1 \\ c_1 \\ c_2 \end{bmatrix} \tag{7}$$

Where:

$\vec{y}_{1i}$ and $\vec{y}_{2i}$ are the $N_{(\alpha+\beta)}$ vectors calculated by Monte Carlo for unitary activity, corresponding to (1-E_1) and (1-E_2), respectively; m and n are the number of data points for y_1 and y_2, respectively.

a is the common intercept; b_1 is the slope for the first curve; c_1 and c_2 are the linear and quadratic coefficients for the second curve, respectively.

3. Results and discussion

A typical experimental gamma spectrum obtained for a (^{243}Am + ^{239}Np) source is compared with Monte Carlo results in Fig. 3. In this plot, the Monte Carlo number of histories in the simulation spectrum was calculated to have the same counting statistics as the experimental spectrum, based on the source activity and gamma-ray efficiency. Therefore, the observed fluctuation in the number of counts for the calculated spectrum is similar to the experimental one. It can be seen that most gamma-ray and X-ray transitions, present in the decay scheme, were identified in the spectrum, when the resolution of the simulated spectrum was set to 1 keV (red points). This resolution was enlarged (green points), in order to compare to the experimental NaI(Tl) spectrum (blue points). A reasonably good agreement can be observed between the experimental and simulated spectra, especially in reproducing the shape distortions at the right of the 106 keV ^{239}Pu gamma-ray peak, due to ^{239}Pu K X-rays, and at the left of the 228 keV ^{239}Pu gamma-ray peak, due to the presence of the 210 keV ^{239}Pu gamma-ray peak. The ambient background was subtracted from the gross counts, resulting in a net spectrum.

Fig. 4 shows a typical 4π(PC) spectrum, obtained with a bias of 1.4 kV. The blue spectrum is experimental and the green one is the Monte Carlo prediction. At the left side, the beta particle and conversion electrons contribution can be seen, as a long tail towards the low amplitude pulses. In the middle region the alpha particle pulses are located. The experimental spectrum has saturated pulses, which were all counted, in order to allow a higher beta particle efficiency. This condition was necessary because a linear amplifier was used and the difference between the electron and alpha pulses was very large. It can be noted that the experimental alpha spectrum has two maxima regions. This can be explained because the 4π(PC) detector has two hemispheres, each one of them with a thin (50 μm) anode with slightly different electrical resistances. This condition results in different gains for each detector hemisphere. In addition, the radioactive source drop is deposited above the film. Therefore, the alpha particles lose part of their energies before reaching the lower hemisphere. The output pulse is the sum of the two signals, producing two maxima in the spectrum.

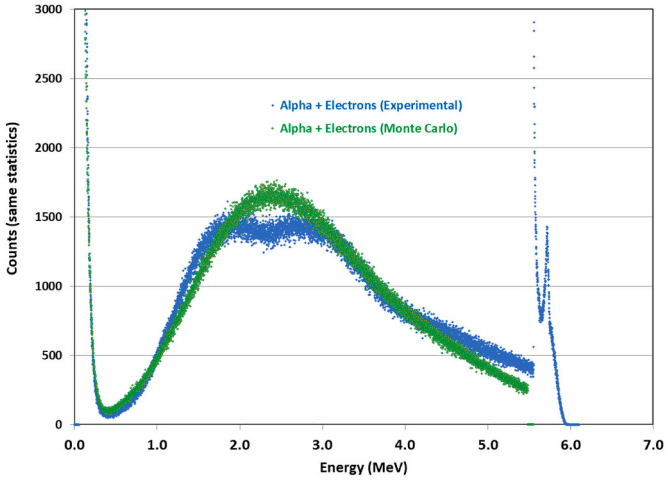

Fig. 4. 4π(PC) detector spectrum applying a bias of 1.4 kV. The blue spectrum is experimental and the green one is predicted by Monte Carlo. The left tail is due to beta particles and conversion electrons. The central region is due to alpha particles. The pulses to the right are due to saturation.

Fig. 5 shows the experimental extrapolation curves obtained by changing the absorber thickness around the radioactive source. The extrapolation value shown corresponds to the sum of ^{243}Am and ^{239}Np equal activities, due to secular radioactive equilibrium. The blue points correspond to the Monte Carlo prediction for the 75 keV gamma-ray window following the ^{243}Am alpha decay. The green points correspond to the (228 + 278) keV gamma-ray window following the ^{239}Np beta decay. The experimental points in both curves follow approximately linear trends with negative slopes, corresponding to the k_1 and k_2 values indicated in Eq. (1). These behavior is reproduced by simulating the contribution of X and gamma-rays in the NaI(Tl) detector window and conversion electrons in the 4π detector. They act as constraints and help to overcome the fluctuations among the experimental points due to statistics or shifts in the gamma-ray windows.

From Eqs. (4) and (5) it was possible to obtain the total specific activity of the solution ($2N_0$) by means of a least square fitting between Monte Carlo calculated values and experimental data. All partial uncertainties were considered and are presented in Table 1. The systematic errors coming from the dead time, resolution time, counting statistics and sample mass were quite small. The main contributions come from fluctuations in the E_1 values, which were observed in some cases, probably due to instabilities in the 4π detector gas pressure or gain variations when the absorber was changed. This effect made necessary to average different measurements with similar E_1 values, as indicated in Fig. 5. Also, uncertainties in the Monte Carlo results may result from mismatch between the theoretical and experimental gamma spectra, mainly in the 75 keV window, where there is an influence from the 106 keV gamma-ray following the beta decay. All these fluctuations contribute to the uncertainty in the fitting, resulting in the main contribution to the total uncertainty. The final result obtained considering all points from the two curves, and applying Eqs. (4) and (5), was 96.21(89) kBq.g^{-1}. Considering the results from the two curves separately, the results for 75 keV and (228 + 278) keV gamma-ray windows were: 95.90(42) kBq.g^{-1} and 96.52(51) kBq.g^{-1}, respectively. The average value from the two extrapolation curves, was 96.16(32) kBq.g^{-1}, showing a lower uncertainty as compared to the first approach. However, in this case, the constraint that the intercept should be the same for both fittings is not obeyed, because it is left as a free parameter. Nevertheless, the two methods apply the Monte Carlo calculation and agree with each other within the estimated uncertainties, indicating that both can be used. These results show that the Monte Carlo modeling was successful and can be useful for predicting the experimental spectra and the extrapolation curve behavior, helping in the final fitting procedure.

4. Conclusions

The primary standardization of a (^{243}Am + ^{239}Np) solution has been accomplished. Monte Carlo modeling by means of an improved version of code ESQUEMA was successfully applied in order to obtain the final activity, by a least square fitting procedure between the experimental data and the Monte Carlo calculation results. The accuracy in the

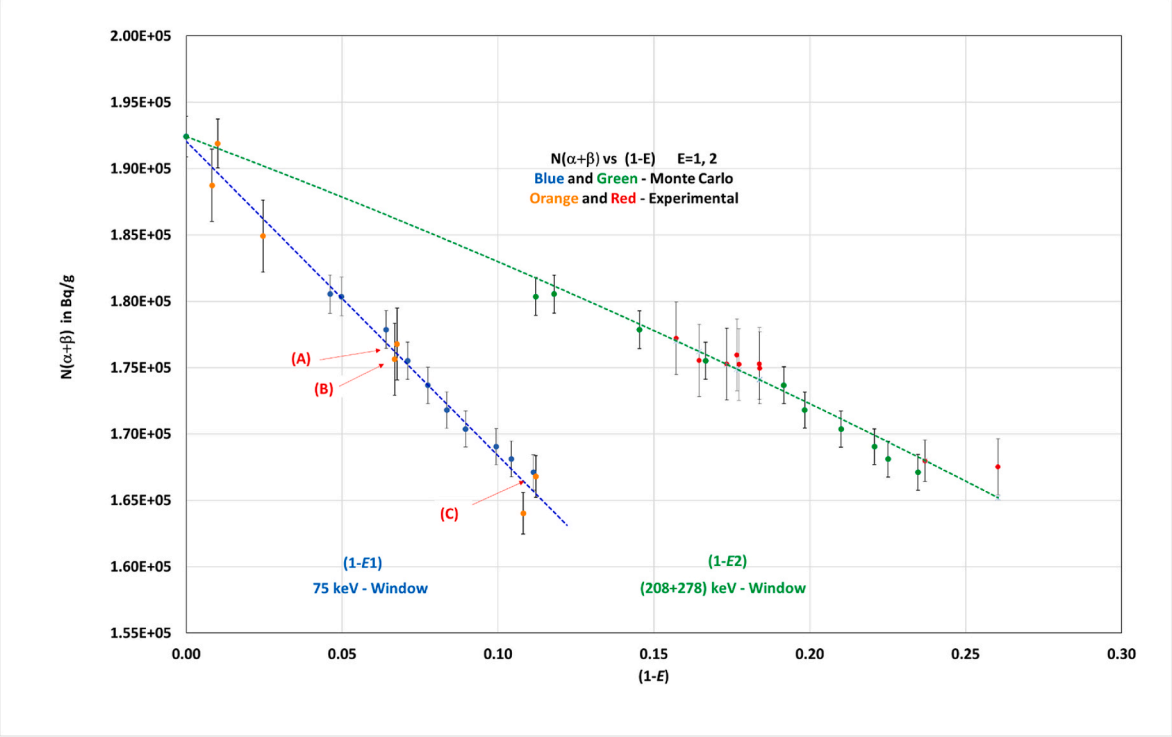

Fig. 5. Extrapolation curve of $N_{(\alpha+\beta)}$ as a function of (1- E). The red and orange dots are experimental points and the blue and green dots are Monte Carlo simulation. Points (A), (B) and (C) correspond to the average of two, six and three experimental values, respectively, for the 75 keV gamma-ray window. For the (228 + 278) keV gamma window, only individual points are shown.

Table 1
Uncertainty budget for the (^{243}Am + ^{239}Np) standardization, in percent ($k = 1$). The extrapolation curve results are shown separately, following Eq. (4). They were averaged in the final result. Eq. (5) corresponds to the second approach: same intercept $2N_0$ for both curves.

Component	Uncertainty (%)	
	^{243}Am	^{239}Np
Monte Carlo statistics (included in fitting)	–	–
Counting statistics (included in fitting)	–	–
Dead time	0.01	0.01
Weight (per sample)	0.10	0.10
Background (included in fitting)	–	–
Decay	0.00	0.00
Resolving time	0.03	0.03
Extrapolation curve fitting - Eq. (4)	0.42	0.52
Extrapolation curve fitting - Eq. (5)	0.89	0.89
Combined Uncertainty - Eq. (4)	0.43	0.53
Combined Uncertainty - Eq. (5)	0.90	0.90

specific activity (0.32 %) was considered satisfactory. The inclusion of a constraint, imposing the same intercept to the two extrapolation curves, did not result in improvement to the overall accuracy. The Monte Carlo modeling was also able to predict reasonably well the experimental gamma-ray spectrum and to identify most of the gamma and X-ray lines present in the NaI(Tl) detector spectrum. It was also helpful in the final fitting because it imposes constraints to the extrapolation curve shapes, allowing reliability to the extrapolation value, even for a limited number of experimental points. The experimental results showed that the inclusion of conversion electrons to the coincidence equations was fundamental, in order to explain the high counting rate even for a lower bias.

CRediT authorship contribution statement

Marina F. Koskinas: Writing – review & editing. **Denise S. Moreira:** Writing – review & editing. **Ione M. Yamazaki:** Writing – review & editing. **Marcelo Colonno:** Methodology. **Renato Semmler:** Writing – review & editing. **Thales S.L. Morais:** Formal analysis. **Mauro S. Dias:** Writing – review & editing.

Declaration of competing interest

This paper does not incur potential conflicts of interest. No human test subjects or animals played a part.

Data availability

Data will be made available on request.

Acknowledgements

The authors would like to acknowledge the National Council for Scientific and Technological Development of Brazil (CNPq) for providing partial funds to the present research work. Grant numbers 304730/2018-1 and 301782/2022-9. Also, the LMN in São Paulo is grateful to the LNMRI (*Laboratório Nacional de Metrologia de Radiações Ionizantes*), from Rio de Janeiro, for providing the (^{243}Am + ^{239}Np) solution. Thanks are also given to Dr. Maurício Moralles, from IPEN, for the valuable discussions on the least square fitting procedure.

References

Bé, M.-M., et al., 2006. Monographie BIPM-5 – table of radionuclides. In: CEA/LNE-LNHB, 91191 Gif-sur-Yvette, France and BIPM, Pavillon de Breteuil, 92312 Sèvres, France, vol. 3. ISBN 92-822-2204-7 (set) et -92-822-2218-7 (Vol. 3). http://www.nucleide.org/DDEP_WG/DDEPdata.htm.

Bé, M.-M., et al., 2008. Monographie BIPM-5 – table of radionuclides. In: CEA/LNE-LNHB, 91191 Gif-sur-Yvette, France and BIPM, Pavillon de Breteuil, 92312 Sèvres,

France, vol. 4. ISBN 92-822-2204-7 (set), 92-822-2230-6 (Vol. 4) et 92-822-2231-4 (CD-Rom). http://www.nucleide.org/DDEP_WG/DDEPdata.htm.
Campion, P.J., 1975. Procedures for Accurately Diluting and Dispensing Radioactive Solutions. Bureau International de Poids et Mesures. Monografie BIPM-1.
Cox, D.R., Isham, V., 1977. A bivariate point process connected with electronic counters. Proc. R. Soc. A 356, 149–160.
Da Silva, C.J., Loureiro, J.S., Delgado, J.U., Poledna, R., Moreira, D.S., Iwahara, A., Tauhata, L., Da Silva, R.L., Lopes, R.T., 2012. Standardization of ^{166m}Ho and ^{243}Am/^{239}Np by live-timed anti-coincidence counting with extending dead time. Appl. Radiat. Isot. 70, 2056–2059.
Dias, M.S., 2010. SCTAC: Version 6. A Code for Activity Calculation Based on Software Coincidence Counting Measurements. IPEN-CNEN/SP. Internal Report.
Dias, M.S., Takeda, M.N., Toledo, F., Brancaccio, F., Tongu, M.L.O., Koskinas, M.F., 2013. Improvements in the Monte Carlo code for simulating 4πβ(PC)–γ coincidence system measurements. Nucl. Instrum. Methods Phys. Res. A 698, 177–184.
Koskinas, M.F., et al., 2016. Standardization of ^{59}Fe by 4π(PC)β–γ software coincidence system. Appl. Radiat. Isot. 109, 386–388.
National Instruments. Online at: http://www.ni.com/lab view/pt/.
ORNL, 2013. Monte Carlo N-Particle Tranport Code System, MCNP6, RSICCComputer Code-Collection. Oak Ridge National Laboratory.
Takeda, M.N., Dias, M.S., Koskinas, M.F., 2005. Application of Monte Carlo simulation to Cs-134 standardization by means of 4π beta–gamma coincidence system. IEEE Trans. Nucl. Sci. 52 (5), 1716.
Toledo, F., Brancaccio, F., Dias, M.S., 2007. Design of electronic system with simultaneous registering of pulse amplitude and event time applied to the 4πβ–γ coincidence method. In: Proceedings of the 2007 International Nuclear Atlantic Conference. INAC, Santos, SP, Brazil, 2007, September 30 to October 5.
Woods, S.A., et al., 1996. Standardisation and measurement of the decay scheme data of ^{243}Am and ^{239}Np. Nucl. Instrum. Methods Phys. Res. A 369, 472–476.
Werner, C.J., et al., 2018. MCNP6. 2 Release Notes. Los Alamos National Laboratory report LA-UR-18-20808.
Yamazaki, I.M., et al., 2018. Disintegration rate and gamma-ray emission probability per decay measurement of ^{64}Cu. Appl. Radiat. Isot. 134, 321-315.
Yamazaki, I.M., et al., 2020. Primary standardization and determination of gamma-ray emission intensities of Ho-166. Appl. Radiat. Isot. 164, 109237.